Multi-property earth model building through integration of Seismic, EM and potential field data with other G&G data: case studies from complex exploration areas.

E. Tartaras, L. Masnaghetti, A. Lovatini, S. Hallinan, M. Mantovani, M. Virgilio, W. Soyer, M. De Stefano and F. Snyder (WesternGeco); Javier Subia (Petrobras); Thierry Dugoujard (Perenco)

This paper was prepared for presentation during the 12th International Congress of the Brazilian Geophysical Society held in Rio de Janeiro, Brazil, August 15-18, 2011.

Abstract

As exploration for hydrocarbon resources moves to increasingly complex geological environments, the integration of multiple physical measurements is needed to build better Earth models.

Seismic has enjoyed a long history as the geophysical workhorse in the oil & gas industry for imaging the subsurface and guiding exploration and development decisions. While this still holds true, it has now become clear that multiple physical measurements are needed to build improved earth models, particularly as exploration for hydrocarbon resources moves to increasingly complex geological environments. Examples of challenges are ultra-deep water exploration (where drilling risks are high), sub-salt and sub-thrust exploration (where seismic imaging faces significant problems).

Non-seismic methods are helping reduce exploration risks and improve development decisions by providing additional information for building a more accurate earth model. Electromagnetic methods measure the EM fields that propagate through the subsurface and provide information (primarily) about the earth's resistivity. This information can be used for structural imaging (e.g., estimating the thickness of conductive sediments underlying a resistive basalt layer) or for reservoir/prospect evaluation/ranking (based on the fact that hydrocarbon-filled rocks are more resistive than water-filled ones). Potential field methods, such as gravity,magnetics, and related gradient measurements, provide density and magnetic susceptibility properties respectively as input to the earth model constraints.

Until quite recently seismic and non-seismic methods were often processed separately and then the final results combined at the interpretation stage. The different "language" used by the two communities and the lack of appropriate software hindered more sophisticated integration. Such comparative interpretations hide advantages that come from closer integration at earlier stages. The level of integration can vary from exploration projects combining different methods at the acquisition and modeling stage to advanced technologies that allow the simultaneous inversion of different datasets. The following case studies show examples of integrated workflows.

The Potiguar integrated exploration project: CSEM prospectivity assessment offshore Brazil

Controlled source EM (CSEM) uses a high-power dipole antenna towed behind a survey vessel, and within 30 meters of the seafloor, to transmit a low-frequency EM field. As these signals propagate through the subsurface, their amplitude and phase are modified depending on the resistivity of the rock units. An array of electromagnetic receivers, deployed on the seabed in a pattern appropriate to the target, measure these characteristics, from which an image of the electrical resistivity structure of the subsurface can be developed. Sediments saturated with salt water have high electrical conductivity (low resistivity) while sediments saturated with hydrocarbons have much higher resistivity. This strong resistivity contrast is detected remotely by the CSEM method, to characterize formations up to 3,000 m below the seabed.

Contrary to its initial marketing as an almost binary method that could be used by itself for decision making, it is now widely accepted that CSEM can provide maximum value when used in combination with other methods. Whereas seismic data can provide continuous information about subsurface structural geology over a large area, CSEM data represents another source of information: powerful at detecting units that are more resistive than the surrounding rocks, but with a low degree of structural resolution. Effective integration with seismic, well logs and other types of data can reduce uncertainty in the interpretation of CSEM data and at the same time build upon its strengths to reduce exploration risk.

This integrated project covered an offshore area of the Potiguar basin, and part of the adjacent Ceará basin, off the north coast of the extreme eastern part of the Brazilian Continental Margin (Figure 1). Onshore, the Potiguar Basin, located mostly in the Rio Grande do Norte State with a small portion in Ceará State, is the second most productive basin in Brazil. Offshore there is currently some production from the nearshore area, but little exploration and no production from the deepwater portion.

This project integrated newly acquired CSEM data with several existing sources of information available in the WesternGeco and Schlumberger portfolio (Lovatini et al., 2010). Extensive knowledge about producing reservoirs in the nearshore and onshore areas of the basin was combined with analysis of natural oil slicks observed at the sea surface, obtained through satellite image processing, as input to a petroleum systems modeling (PSM) study. Other inputs included well log data, reprocessed seismic data, and geochemical analysis of oil samples. The geochemical analysis included identification of biomarkers, which can help determine the thermal maturity or the temperature of burial, and can

provide indications of the type of source rock, migration path, and alteration history of hydrocarbon deposits.

A 2D marine seismic data survey acquired in 1999, which had originally been processed to prestack time migration, was reprocessed using surface-related multiple elimination (SRME) and prestack depth migration (PSDM). This was interpreted to provide regional scale horizons, which were used as input, along with other geological and geochemical information, for a petroleum system model of the whole basin. The interpretation highlighted several possible structural and stratigraphic traps. These, and the sea surface oil slick locations, were used to identify areas where CSEM data would most likely provide additional information to reduce exploration risk.

Four separate prospects (all outside currently held concessions) were finally chosen following analysis of their CSEM detectability and seismic characteristics. The CSEM survey comprised more than 250km of towlines recorded by 136 multicomponent EM receivers. After the initial onboard processing, the following inversion and interpretation workflow was applied to the CSEM data sets:

- Qualitative interpretation
- 1D anisotropic inversions, constraining the thicknesses with the seismic horizons to derive horizontal and vertical background resistivities
- Up-scaling to 2D and 3D resistivity volumes (Figure 2)
- Forward modeling to assess the background model validity
- 2.5D anisotropic inversions
- 3D anisotropic inversions
- Integration with seismic and other data using Petrel* seismic-to-simulation software.

All the 3D inversions (Mackie et al. 2007) in this project included both inline and broadside data, and utilized multiple frequencies to improve inversion sensitivity and depth resolution. Integration of the resistivity volumes obtained through 3D anisotropic inversions of the five CSEM datasets provided a new approach to better understand the earth model for the PSM and prospectivity study of the offshore Potiguar basin (Figure 3 and Figure 4). The additional information can be used to guide further analysis and interpretation of prospective areas on the seismic data, highlighting the value of using EM techniques as a prospectivity ranking tool. More importantly, the whole integrated workflow demonstrates how the early integration of other data (in this case seismic, well, and satellite data) can help design a better CSEM survey and obtain a better inversion result which, in turn, helps in interpreting the original seismic image.

SubAndean Foothills, SE Bolivia: MT survey to help delineate gas reservoir constraining resistivity models with well logs to test working structural models

The seismic imaging issues of the near-vertical foldbelt structures in this region have increased the risks of drilling to the deep gas reservoir targets. The host structures are often displaced laterally with respect to the outcropping anticline structures, located below thrust faults (Ravaut et al., 2002).

Well log resistivities (Figure 5) show a marked resistivity increase at the top of the relatively clean reservoir hosting sandstones of the Middle Devonian, compared to lower formation resistivities of the shallower formations. The contrast is sufficient for these deep structures to be mapped by surface magnetotelluric (MT) surveys. A 3D MT survey comprising 165 MT soundings at 500 to 1000m spacing along dip lines, spaced 2 to 3km apart, was carried out over the present prospect, prior to completion of drilling by Petrobras.

Figure 6 shows an overlay of two MT inversion model approaches. The line contours represent the unconstrained (blind) inversions, completed before drilling, and the later constrained inversion models. For the latter, where the working geological model and resistivity logs (supplied by Petrobras) were integrated to control the geometrical “layered” structure and resistivity of the starting model, the data were inverted for resistivity perturbations required to fit the observed MT data.

The blind and the constrained inversions both show a resistive core offset from the well locations, consistent with the structure and resistivity logs from the wells (Figure 6).

The present case study shows how the integration of different geophysical measurements at different stages of the interpretation workflow improved the mapping of deep gas reservoirs in an area of challenged seismic imaging, and helped reduce the drilling risk.

Salt detection in Gabon by seismic-gravity simultaneous joint inversion

Many examples from around the world indicate that conventional ray tomography can fail in the presence of salt. It is generally accepted that base-salt reflections are often distorted by complex salt bodies, and if a background model based on seismic data cannot accurately reconstruct the salt, it is not possible to update that model via ray tomography. As a secondary effect of this, distortion propagates vertically, and sub-salt marker horizons are also likely to be poorly imaged (Figure 7). Tomography based on interpretation of seismic data is likely to fail because salt bottoms are often difficult to interpret, broken, or mixed with migration artefacts. For the same reason, dip-field tomography is also unlikely to deliver the required results.

Gravity provides a key indicator of salt in regions with this type of seismic response. The method can discriminate low density salt in a lateral sense, and when combined with seismic imaging for vertical resolution, it is possible to locate the position of the salt, even if it cannot resolve

its shape. By resolving both velocity and density simultaneously, joint inversion can detect where salt exists inside a particular multi-parameter model as it results in a sharp violation of accepted background velocity-density relationships such as Gardner's rule.

Hydrocarbon exploration in the South Gabon sub-basin has produced many large oil discoveries; however, developing accurate depth maps of its pre-salt objectives remains elusive. Vertical relief of the base-salt horizon—the ultimate seal—is often less or equal to the uncertainty inherent in constructing the depth model. Established oilfields will usually have sufficient well data to build depth maps that are more accurate than maps based on seismic data, but depth maps for exploration areas often rely solely on seismic data. Perenco hypothesized that gravity data could be utilized in an exploration area to enhance the imaging of pre-salt seismic reflectors by providing additional input for prestack depth migration (PSDM). As a test, two vintage 2D seismic lines were reprocessed utilizing simultaneous joint inversion (SJI) technology developed by WesternGeco (Colombo, Mantovani et al. 2007, Colombo et al. 2007, Colombo et al. 2008). The results of the test encouraged Perenco and its partner to pursue application of the workflow to a complete 2D seismic dataset covering the area of interest.

The study area has thick Barremian rift-phase Dentale formation sands and shales overlain by discordant Gamba sandstones (Mantovani and Dugoujard, 2011). This sequence is overlain by the Aptian Ezanga evaporitic sequence, which provides the ultimate top seal for Gamba or Dentale sandstone reservoirs. A thick, complex, Madiela carbonate layer forms most of the rest of the overburden. Changes in the facies and thickness of the Madiela formation — both vertically and laterally — lead to a poorly defined velocity model for this layer.

Airborne gravity data were acquired along North-South lines spaced 250 m apart and East-West tie lines were acquired at 2,500 m spacing. After data levelling and processing, WesternGeco and Perenco worked together to create a realistic input model for the joint inversion. Joint inversion was used as a sensitivity test on the seismic interpretation and allowed elimination of non-geological scenarios while preserving geophysically plausible scenarios (Mantovani and Dugoujard, 2011).

The SJI process attempts to fit simultaneously both gravity and seismic datasets by finding the best velocity and density models, subject to two sets of constraints. A first set of constraints imposes structural similarity among the gravity and velocity models, as the subsurface anomalies are inverted from the seismic or gravity response of the same subsurface formations and are therefore expected to have a similar distribution. A second set of constraints maps the velocities into densities and vice-versa by imposing a relationship from petrophysical properties. Such a relationship may consist of empirical or analytic functions such as the Gardner's equation or user-defined functions derived from well logs, as in this case for the Ezanga salt.

Salt represents an exception for the standard SJI in terms of the velocity-density relationship. The exploration play can be described as if inside a uniform space where the Gardner rule is valid, but a single body deviates from this rule and follows a well derived velocity-density trend instead. If a correct interpretation of the contours is used, the exception effect becomes invisible to the system and SJI can operate, minimizing the residuals as usual. If the salt interpretation is not correct, the anomalous log-derived velocity-density trend that replaces the Gardner rule (Gardner et al., 1974) is misplaced, and the SJI exhibits a set of known artefacts. The interpretation is then interactively adjusted until these artefacts are removed. A new iteration of SJI is then run to prove the salt interpretation, and so on. The asymptote to this process is the production of the correct interpretation. As a secondary effect, SJI can derive the correct velocity and density model.

Simultaneous joint inversion is therefore able to detect a bad salt interpretation, and can lead the interpreter towards correct salt boundaries. This is true even in cases, as in the example described, where not much information from the seismic section or velocity distribution is available. The salt detection workflow consists of fixing the expected non-Gardner trend into an interpreted salt, and then inverting for the salt shape.

Where previous interpretation within the pre-salt section of this South Gabon sub-basin was limited by poor imaging, particularly beneath salt mounds (Figure 7), analysis of the reprocessed seismic lines provided improved continuity (Figure 8). The new data validate correlation of the Dentale formations between wells, and allow a better understanding of its faulting and structure. Base-salt depth might not yet be as accurate as desired, but future processing of a dense network of lines can be expected to pinpoint relative base salt highs.

3D simultaneous joint inversion of seismic and magnetotelluric data for sub-salt imaging in the Gulf of Mexico

The numerous coalescing allochthonous salt canopies that cover potential reservoir structures are particular challenges to deepwater Gulf of Mexico exploration. Properly interpreting these salt structures is a key to understanding and creating accurate tomographic velocity models, which in turn, are necessary to properly position and image the subsalt targets. By better integrating geology and geophysics, we are improving our models. This is particularly important in the Green Canyon-Garden Banks-Keathley Canyon-Walker Ridge areas where salt complexity is challenging, even with the latest wide-azimuth acquisition and processing methods. Various approaches have been proposed (Gallardo and Meju, 2004; Colombo and De Stefano, 2007) for multi-domain and multi-measurement integration, both in processing and interpretation. Here we show how to use 3D SJI of seismic and MT data to better define the base salt and improve sub-salt imaging (Virgilio et al., 2010).

As described in the Gabon case study, SJI inverts simultaneously seismic and non-seismic data, as opposed to inverting each dataset separately. As stated before, the links between the different domains in the SJI algorithm are either geometrical or empirical. Geometrical links encourage different 3D models to have similar

geometrical variations, by means of cross-gradient computation of contours. Empirical laws link the absolute values of velocity and resistivity by means of well-known equations adapted and tuned for a specific project.

Marine magneto-telluric MMT data were acquired with an array of seabed receivers recording horizontal electric and magnetic fields to provide the estimate of the full MT impedance tensor. The MMT time series were then processed using a robust remote reference algorithm. The processed data were found to be of good quality in the expected frequency range. For the 3D SJI proof of concept in the northern Walker ridge area, we started from an existing seismic reflection tomographic model from which we removed a portion of the salt (Figure 9, top right) to obtain the initial velocity model. Several iterations of targeted 3D SJI with reflection seismic and MMT data were run to obtain the final SJI velocity model (Figure 9 , bottom right) together with its corresponding resistivity model. The bottom left image in Figure 8 shows how the 3D SJI has led to a new 3D interpretation of the allochthonous salt base (colored) and positioning of the autochthonous top salt (blue).

Figure 10 shows old wave-equation migration image overlaid by the velocity obtained with the old reflection tomography (left), and the SJI velocity model (middle: updates from initial model - blue is low and red is high update) with interpretations (right). The low-velocity zone immediately below the salt has been useful when interpreting the boundary salt sediments: the white horizon is the interpretation of the allochthonous salt from the single-domain seismic approach, the red is the SJI interpretation of the same formation (the difference between the interpretations reaches 700 m), the blue is the SJI interpretation of the top autochthonous salt, consistent with the indication of a deep high velocity coming from SJI. Note that the high velocity of autochthonous salt is absent in the single-domain velocity model (left) and present only in the SJI velocity model (middle and right) given the MMT capability of seeing the resistive salt anomaly.

The 3D SJI example of seismic and MMT data over the northern Gulf of Mexico has led to new interpretation of the allochthonous and autochthonous salt. Simultaneous Joint Inversion reduces inversion uncertainties, and defines a new strategy for sub-salt interpretation; thereby, enhancing the role of non-seismic methods as supporting complex seismic depth imaging.

Conclusions

The presented case studies clearly show the value EM and potential field data can bring to building a more accurate model of the subsurface. However, to maximize this value, it is imperative that these data are not interpreted in isolation but integrated as far as possible, and as early as possible, with other available G&G data. The integration can range from combining various datasets in a cooperative interpretation to actually using simultaneous joint inversion to obtain a single earth model from two different datasets. In all cases the final goal is to reduce the risk inherent in all exploration and development decisions.

Acknowledgments

The authors thank the Gabon Direction Generale des Hydrocarbures (DGH), Perenco, Petrobras and WesternGeco for permission to present this work.

References

Colombo, D. and De Stefano, M. [2007] Geophysical modelling via Simultaneous Joint Inversion of Seismic, Gravity and Electromagnetic data: application to Pre-Stack Depth Imaging. *The Leading Edge*, March 2007, 326-331.

Colombo D., Mantovani, M., De Stefano, M., Garrad, D., and Al Lawati, H. [2007] Simultaneous Joint Inversion of Seismic and Gravity data for long offset Pre-Stack Depth Migration in Northern Oman, *Canadian SEG*, 2007, Calgary.

Colombo, D., Cogan, M. Hallinan, S., Mantovani, M., Virgilio,M., and Soyer, W. [2008] Near Surface P-velocity Modeling by Integrated Seismic, EM, and Gravity Data: Examples from Middle East, *First Break*, 26, 91–102.

De Stefano, M. and Colombo, D. [2006] Geophysical modeling through simultaneous Joint Inversion of Seismic, Gravity and Magnetotelluric data. *Integration of Seismic and Electromagnetic Measurements Workshop*, SEG 2006, 2006.

Gallardo, L.A. and Meju, M.A. [2004] Joint 2D resistivity and seismic inversion with cross-gradients criterion: *Journal of Geophysical Research*, 109, 1-11.

Gardner, G., Gardner, L. and Gregory, A. [1974] Formation velocity and density – the diagnostic basics for stratigraphic traps. *Geophysics*, 39(6), 770-780.

Lovatini, A., Myers, K., Watterson, P. and Campbell, T. [2010] An integrated approach to exploration data in the Potiguar Basin, offshore Brazil. First Break, 28(5), 55-59.

Mantovani, M. and Dugoujard, T. [2011] Salt detection and interactive interpretation by seismic-gravity simultaneous joint inversion: *First Break* (submitted).

Ravaut, P., Russell, S., Mallard, P., Ballard, J.-F., Watts, M.D., Mackie, R. and Hallinan, S. [2002] 3D Magneto-tellurics for imaging a Devonian reservoir (Huamampampa) in the southern Sub-Andean basin of Bolivia, SEG Expanded Abstracts 21, 2417-2421.

Virgilio, M., De Stefano, M., Re, S., Golfè Andreasi, F. and Snyder, F.F.C. [2010] Simultaneous Joint Inversion of Seismic, Gravity and EM data for Sub-Salt Depth Imaging in Gulf of Mexico, *EAGE paper K045*, Barcelona.

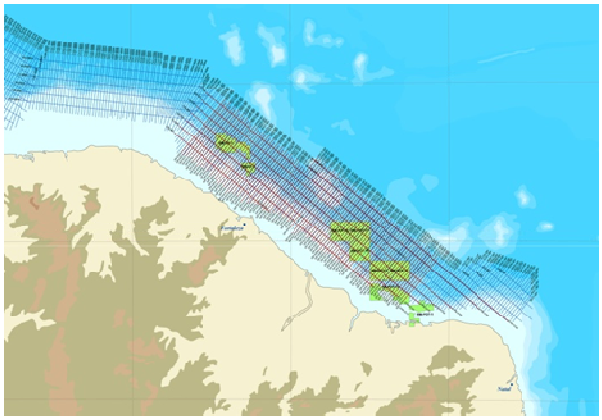

Figure 1; The Potiguar-Cearà basin, N.E. Brazil

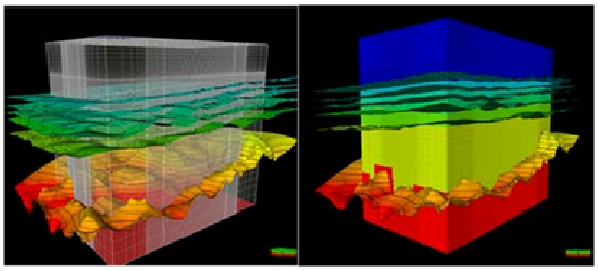

Figure 2; Example of 3D inversion mesh generation using the horizon surfaces (left) and after population with resistivity (right).

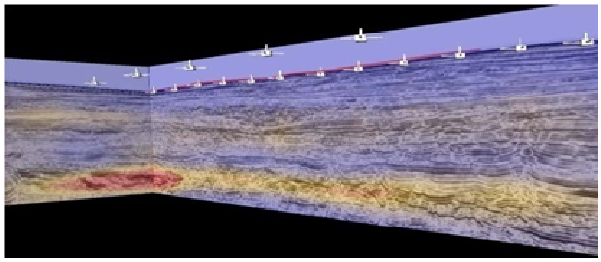

Figure 3; Vertical resistivity output volume co-rendered with seismic sections. White symbols indicate receivers and the red line the source path.

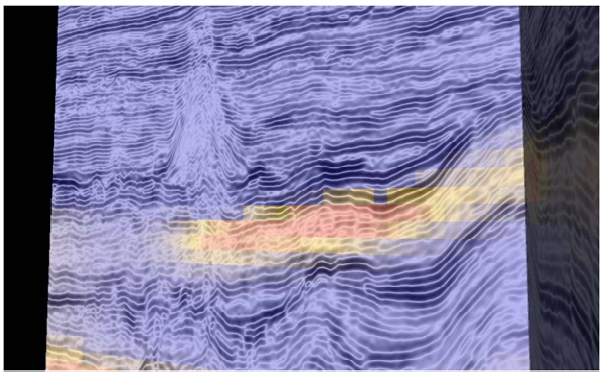

Figure 4; Vertical resistivity output volume co-rendered with seismic sections. The lack of a resistivity anomaly in the chimney-like seismic feature discourage its interpretation as a volcanic feature, whereas the resistivity increase nearby may complement the interpretation of seismic data.

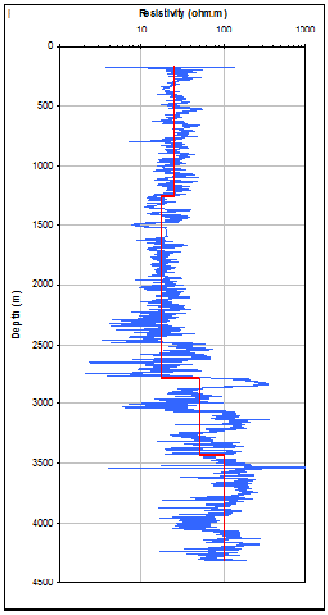

Figure 5; Resistivity log example showing the significant increase at depth.

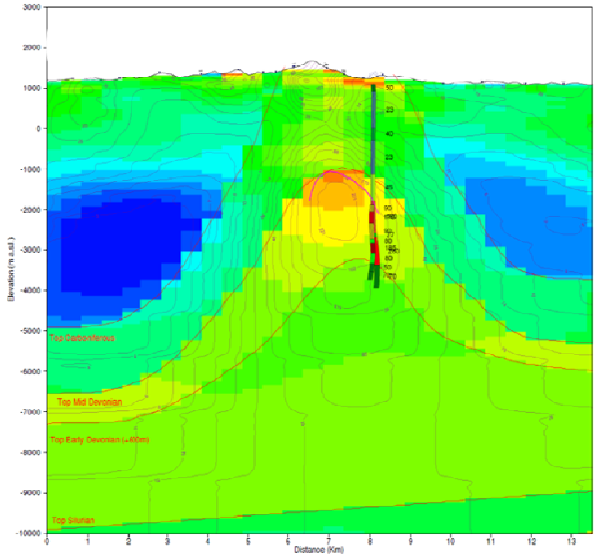

Figure 6; Dip line resistivity cross section comparing constrained 3D resistivity inversion (color grid), unconstrained (blind) 3D inversion (line contours), surfaces interpolated from working structural model to construct constrained starting resistivity model, and condensed well log resistivities. Short purple line is top of axial resistor picked from 3D blind inversion.

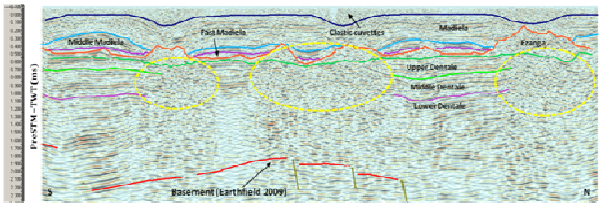

Figure 7; Vintage PSTM seismic test line 1. Note poor pre-salt imaging below salt mounds.

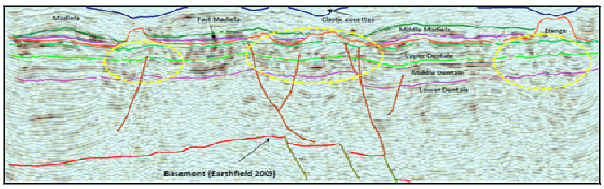

Figure 8; PSDM seismic test line 1 converted back to time.

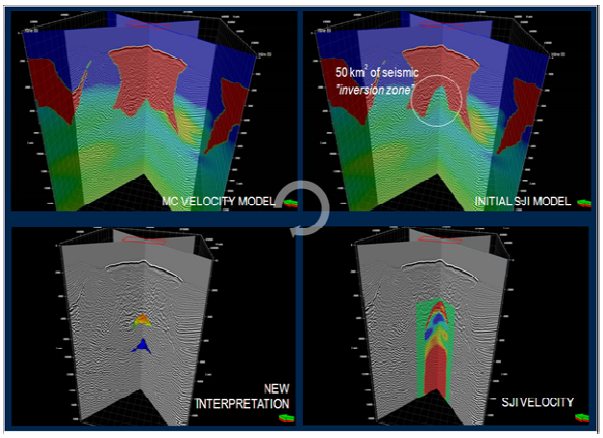

Figure 9; 3D views of velocities (colored) and seismic (black and white) overlays.

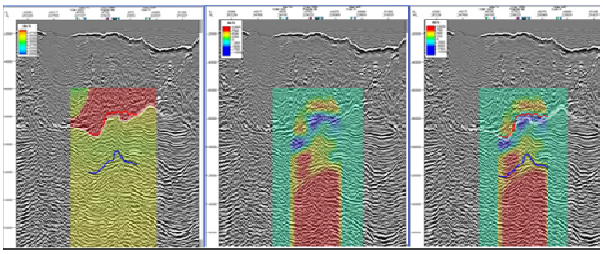

Figure 10; old wave-equation migration image overlaid by the velocity obtained with the old reflection tomography (left), and the SJI velocity model (middle: updates from initial model - blue is low and red is high update) with interpretations (right)